

# Mechanistic Analysis of the Observed Linear Free Energy Relationships in p21<sup>ras</sup> and Related Systems<sup>†</sup>

T. Schweins<sup>\*,‡,§</sup> and A. Warshel<sup>\*,‡</sup>

Department of Chemistry, University of Southern California, Los Angeles, California 90089-1062, and Max-Planck-Institut für molekulare Physiologie, Abteilung Strukturelle Biologie, Rheinlanddamm 201, 44139 Dortmund, Germany

Received May 10, 1996; Revised Manuscript Received August 26, 1996<sup>®</sup>

**ABSTRACT:** Previous studies of the GTPase reaction catalyzed by p21<sup>ras</sup> have indicated that the logarithm of the observed reaction rate and the pK<sub>a</sub> of the bound GTP are correlated by the Brønsted relationship  $\log(k_{\text{cat}}) = \beta \text{p}K_{\text{a}} + A$ . While most of the Ras mutants display a Brønsted slope  $\beta$  of 2.1, a small set of oncogenic mutants exhibit a  $\beta$  of  $\gg 1$ . On the other hand, it was found that the corresponding Brønsted slope for the GTPase reaction of p21<sup>ras</sup> in the presence of GTPase Activating Protein (GAP) is about  $\beta = 4.9$ . The present work explores the basis for such linear free energy relationships (LFERs) in general and applies these concepts to p21<sup>ras</sup> and related systems. It is demonstrated that the optimal way to analyze LFER is by using Marcus type parabolas that represent the reactant, intermediate, and product state of the reaction in a relevant energy diagram. The observed LFER is used to analyze the actual free energy surface and reaction path of the intrinsic GTPase reaction in p21<sup>ras</sup>. From this, a model reaction profile can be constructed that explains how a LFER can arise and also how the different observed Brønsted coefficients can be rationalized. This analysis is augmented by solvent isotope effect studies. It is pointed out that the overall activation barrier reflects the energy of the proton transfer (PT) step, although this step does not include the actual transition state of the hydrolysis reaction. The proposed GTP as a base mechanism is compared to a recently proposed reaction scheme where Gln61 serves as a proton shuttle in a concerted mechanism. It is shown by unique energy considerations that the concerted mechanism is unlikely. Other alternative mechanisms are also considered, and their consistency with the observed LFER and other factors is discussed. Finally, we analyze the observed LFER for the GTPase reaction of p21<sup>ras</sup> in the presence of GAP and discuss its relevance for the mechanism of GAP activation.

The preceding work (Schweins et al., 1996) has used protein engineering methods to analyze the effects of a pK<sub>a</sub> change of the terminal GTP–phosphate bound to p21<sup>ras</sup> on the reaction rate. The corresponding Brønsted plot establishes the existence of a linear correlation between these two parameters. The higher the pK<sub>a</sub> of the  $\gamma$ -phosphate and the stronger its proton abstraction potential, the faster the reaction rate at neutral pH. Thus, this study exhibits a linear free energy relationship (LFER)<sup>1</sup> between the free energy of activation,  $\Delta G^\ddagger$ , of this reaction and the pK<sub>a</sub> of the  $\gamma$ -phosphate of the protein-bound GTP.

The observed LFER as well as theoretical and structural studies indicate that the substrate of the reaction, the GTP itself, plays a central role in the proposed reaction scheme by acting as a base catalyst (Schweins et al., 1994, 1995). According to this proposal, the GTP hydrolysis in p21<sup>ras</sup> is initiated as shown in Figure 1 by the abstraction of a proton from the catalytic water molecule by the  $\gamma$ -phosphate of protein-bound GTP. This yields a nucleophilic hydroxide ion (state II) that subsequently attacks the protonated

$\gamma$ -phosphate and creates the proposed trigonal bipyramidal transition and intermediate state (state III), respectively. With GDP as the leaving group, this pentacoordinate intermediate finally breaks into the reaction products phosphate and GDP (state IV). This work attempts to further examine the above proposal, focusing on the observed LFER and its mechanistic implications.

A traditional way of probing the potential surface in reactions of simple organic molecules is the use of a LFER. Very often, one finds empirical linear relationships between activation free energies ( $\Delta G^\ddagger$ ) and equilibrium free energies ( $\Delta G^\circ$ ) for the reactants and products or some intermediate. The validity of such relationships in electron transfer and for chemical processes in solutions has been the subject of many studies [e.g. Leffler and Grunwald (1963), Marcus (1964), Albery (1980), Kreevoy & Kotchevar (1990), and Warshel (1991)]. Experimental studies (Fersht et al., 1986; Kirsch et al., 1989) as well as theoretical studies (Warshel, 1984; Warshel et al., 1994) indicate that such relationships are also valid in proteins and can be used as a powerful tool to correlate the catalytic power of enzymes with their structure.

In this work, it is demonstrated that the optimal way to analyze a LFER for chemical reactions in enzymes and solution is the use of a modified Marcus relationship, representing the reaction by intersecting parabolas. These parabolas correspond to resonance structures that describe the reacting fragments in the reactant, intermediate, and

<sup>†</sup> T.S. gratefully acknowledges support by an Otto-Hahn fellowship from the Max-Planck-Society. A. Warshel acknowledges support by DOE Grant DE-FG03–94ER61945 and Tobacco Grant 4RT-0002. The work at the Max-Planck-Institut in Dortmund was supported by Bayer Inc. (to T.S. and A. Wittinghofer).

\* E-mail: warshel@invitro.usc.edu and tomas@usc.edu.

<sup>‡</sup> University of Southern California.

<sup>§</sup> Max-Planck-Institut für molekulare Physiologie.

<sup>®</sup> Abstract published in *Advance ACS Abstracts*, October 15, 1996.

<sup>1</sup> Abbreviations: LFER, linear free energy relationship; GAP, GTPase activating protein; PT, proton transfer; TS, transition state.

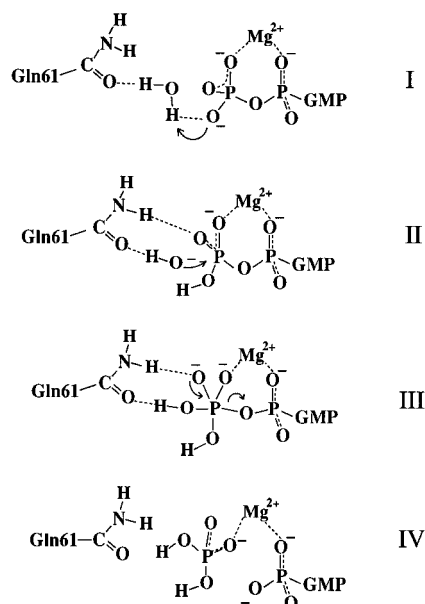


FIGURE 1: Reaction sequence in the GTP as a base mechanism. In this mechanism, the GTP acts as a general base for its own hydrolysis. The proton transfer from the nucleophilic water to the phosphate activates the nucleophile and increases the electrophilicity of the  $\gamma$ -phosphate. This step reduces the negative charge on the phosphate and makes it easier for the negative nucleophile to attack. The GTP as a base mechanism was proposed first for p21<sup>ras</sup> as the result of a computer modeling study (Schweins et al., 1994) and supported by experimental studies (Schweins, 1995). Sigler and co-workers adopted this mechanism for transducin (Sondek et al., 1994), and Fisher et al. (1995) proposed a related ATP as a base mechanism for myosin.

product state of the reaction. The observed LFER for the GTPase of p21<sup>ras</sup> is used to analyze the reaction mechanism and to probe the corresponding free energy surface for this reaction. Further, with the help of this model reaction profile, the different observed Brønsted slopes can be rationalized. It is illustrated that the reaction mechanism of Ras-related proteins that exhibit different reaction rates as well as the GAP-stimulated reaction can be explained with the same GTP as a base mechanism that was proposed for the intrinsic reaction of p21<sup>ras</sup>.

#### How Can Linear Free Energy Relationships Arise?

Chemical reactions in enzymes and solution very often exhibit an empirical relationship between the observed reaction rate,  $k$ , and the corresponding equilibrium constant,  $K$  [e.g. Leffler and Grunwald (1963)]. If the reaction mechanism and the rate-limiting step are unchanged for a series of mutants, a linear plot with a slope of  $\alpha$  may be obtained when  $\log(k_{\text{cat}})$  is plotted as a function of  $\log(K)$ . Such a correlation is derived in a phenomenological way from the relationship

$$k = AK^{\alpha} \quad (1)$$

where  $A$  and  $\alpha$  are constant over a certain range. When eq 1 holds, the plot of  $\log(k)$  against  $\log(K)$  is a straight line of slope  $\alpha$  (eq 2).

$$\log(k) = \alpha \log(K) + B \quad (2)$$

with  $B = \log(A)$ . For the specific case of a proton transfer reaction,  $\log(K)$  can be approximated by the difference between the  $\text{p}K_{\text{a}}$  of the donor (D) and the acceptor (A). Thus, we arrive at a relationship for this class of reactions that is

well-known as the Brønsted law

$$\begin{aligned} \log(k) &= \alpha(\text{p}K_{\text{a}}^{\text{A}} - \text{p}K_{\text{a}}^{\text{D}}) + B \\ &= \alpha \Delta \text{p}K_{\text{a}}^{\text{AD}} + B \end{aligned} \quad (3)$$

and for the corresponding difference between mutant and wild type protein we obtain

$$\Delta \log(k) = \alpha \Delta \Delta \text{p}K_{\text{a}}^{\text{AD}} \quad (4)$$

The Brønsted law relates the rate of a reaction directly to the corresponding equilibrium that is determined by the  $\text{p}K_{\text{a}}$  difference between the proton donor and the acceptor. From transition-state theory, we know that  $\log(k)$  is proportional to the free energy of activation,<sup>2</sup>  $\Delta G^{\ddagger}$  (eq 5), while from equilibrium thermodynamics, it is known that  $\log(K)$  is proportional to the equilibrium free energy,  $\Delta G^{\circ}$  (eq 6).

$$\log(k) = \frac{-\Delta G^{\ddagger}}{2.303RT} + c \quad (5)$$

$$\log(K) = \frac{-\Delta G^{\circ}}{2.303RT} \quad (6)$$

By substituting eqs 5 and 6 in eq 2, we obtain an equation that illustrates the linear relationships between the free energies of activation and equilibrium:

$$\Delta G^{\ddagger} = \alpha \Delta G^{\circ} + C \quad (7)$$

where  $C$  is a constant and  $\alpha$  the LFER correlation coefficient. For the corresponding difference between the mutant and the wild type protein, we obtain in analogy to eq 4

$$\Delta \Delta G^{\ddagger} = \alpha \Delta \Delta G^{\circ} \quad (8)$$

Note that the LFER presented in the preceding paper was obtained by titrating the GTP bound to p21<sup>ras</sup>. In this case, the proton donor is in fact a  $\text{H}_3\text{O}^{+}$  molecule of the bulk solvent (generated by the addition of diluted acid). However, according to the proposed mechanism, GTP abstracts a proton from a neutral water molecule which is located in the active site and the nucleophilic  $\text{OH}^{-}$  ion is generated (see Figure 1). Thus, the experimentally determined  $\Delta \text{p}K_{\text{a}}^{\text{A}}$  is not exactly identical to the  $\Delta \Delta \text{p}K_{\text{a}}^{\text{AD}}$  that defines the actual energetics for the proposed proton transfer (PT) step of the GTPase reaction. Nevertheless, these two entities are closely related. The value of the relevant LFER correlation coefficient  $\alpha$  is slightly larger than the actual observed Brønsted slope  $\beta$  (see footnote 3). In the subsequent parts of this paper, we refer for simplicity always to the experimentally determined LFER correlation coefficient  $\beta$ . The final conclusions that are drawn for the mechanism of p21<sup>ras</sup> remain unchanged. However, the reader should keep in mind that the experimentally observed LFER slopes  $\beta$  are expected to be smaller than the closely related correlation coefficient  $\alpha$  that is defined by the actual energetics of the proposed mechanism.

With eq 8 in mind, we now may ask what is the reason for a linear correlation between the free energy of activation,

<sup>2</sup> More rigorous treatments denote the activation free energy by  $\Delta g^{\ddagger}$  rather than  $\Delta G^{\ddagger}$  [see Warshel (1991) for a detailed explanation]. However, for simplicity, we use in this work  $\Delta G^{\ddagger}$  instead of  $\Delta g^{\ddagger}$  when we refer to the free energy of activation of a chemical reaction.

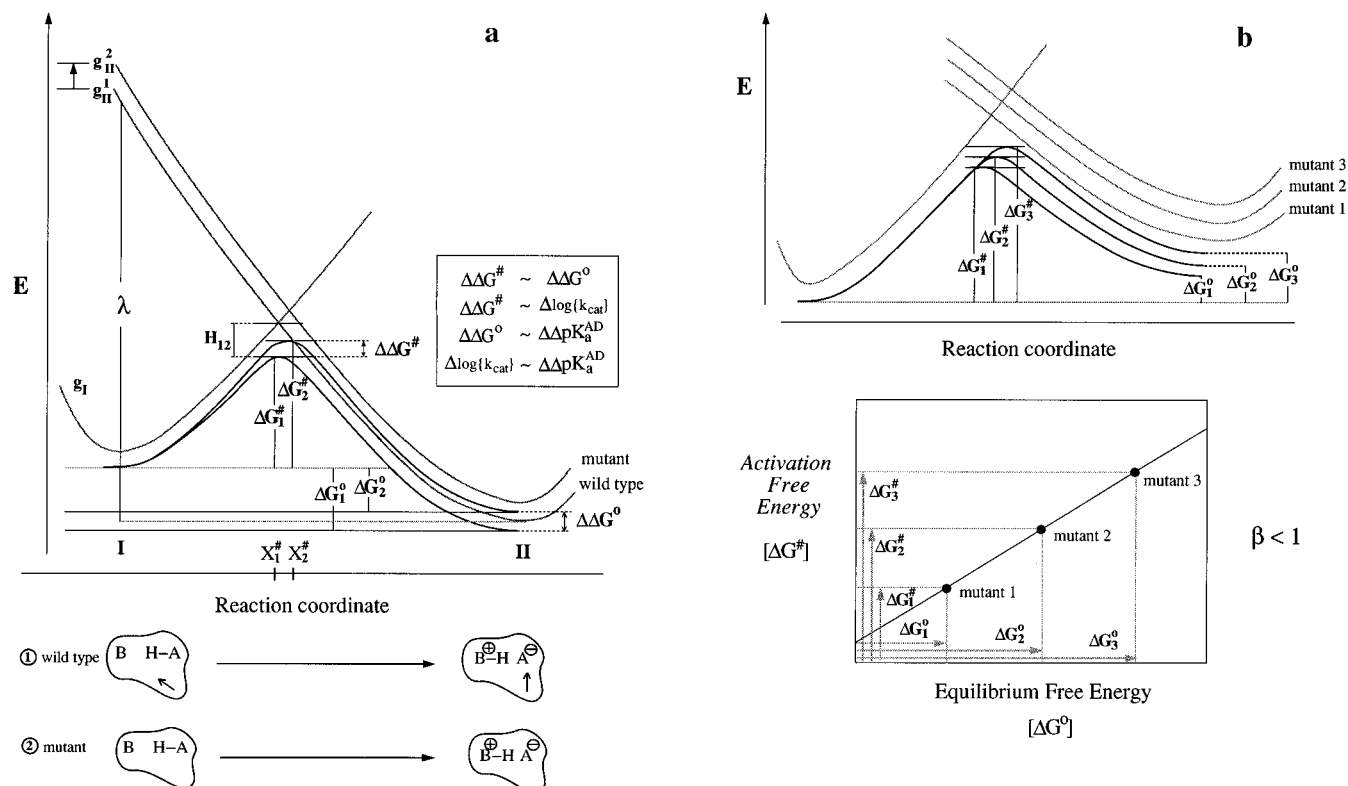


FIGURE 2: (a) Schematic description of the relationship between the free energy difference,  $\Delta G^{\circ}$ , and the activation energy in a two-state model. This figure illustrates how a shift of the free energy function  $g_{II}$  by  $\Delta \Delta g_{II}^{\ddagger}$  (which changes  $g_{II}^{\ddagger}$  to  $g_{II}^{\ddagger\prime}$ ) changes  $\Delta G^{\ddagger}$  by a similar amount ( $\Delta \Delta G^{\ddagger}$ ). If, for example, a dipole in a protein's active site that exclusively increases the energy of state II is mutated, one will find that the equilibrium free energy of this reaction,  $\Delta G^{\circ}$ , increases (since state II is destabilized). As a result of this, the activation free energy,  $\Delta G^{\ddagger}$ , increases and therefore the rate constant decreases. Note that for proton transfer reactions  $\Delta \Delta G^{\circ}$  is proportional to  $\Delta pK_a^{AD}$  (the  $pK_a$  difference between proton acceptor and donor) and  $\Delta \Delta G^{\ddagger}$  according to transition-state theory proportional to  $\Delta \log(k_{cat})$ . Therefore,  $\Delta \Delta G^{\ddagger}$  is as a result of the LFER proportional to  $\Delta \Delta G^{\circ}$  and thus indirectly also to  $\Delta pK_a^{AD}$ . The parameter  $\lambda$  is the well-known reorganization energy, which is used in the modified Marcus relationship of eqs 9 and 10.  $H_{12}$  is the term that describes the resonance mixing of the two interacting states and thus represents the difference between the parabolas and the actual free energy surface of the corresponding chemical reaction. Note that the validity of using Marcus type parabolas to describe a LFER is not restricted to changes that solely affect state II in a two-step reaction. The same result would be obtained if the energy of state I is affected or if one has to consider a three-step reaction. (b) Relationship between the potential surface of a reaction and a LFER plot. It is shown how a set of three mutants that have a different energetic effect on state II of the reaction lead to a LFER between the activation free energy,  $\Delta G^{\ddagger}$ , and the corresponding equilibrium free energy,  $\Delta G^{\circ}$ . Note that the correlation coefficient  $\beta$  cannot exceed 1 if one assumes that the curvature of the parabolas does not change.

$\Delta G^{\ddagger}$ , and the equilibrium free energy,  $\Delta G^{\circ}$ . The original use of the LFER [e.g. Hammett (1937), Leffler and Grunwald (1963), and Jencks (1969)] was primarily based on empirical observations. Subsequently, it was shown by Marcus (1964)

<sup>3</sup> The free energy,  $\Delta G^{\circ}$ , of the proposed PT step of the GTP hydrolysis reaction involves the difference between the  $pK_a$  of the  $\gamma$ -phosphate of the GTP molecule and the  $pK_a$  of the proton donor (the active site water molecule). Since only the  $pK_a$  of the  $\gamma$ -phosphate is measured experimentally, we have to try to relate the catalytic rate constant to this  $pK_a$  rather than to  $\Delta G^{\circ}$ . In most cases, it is expected that mutational effects that stabilize the negative charge of the  $\gamma$ -phosphate would also stabilize the negative charge of the nucleophilic  $OH^-$  ion generated by the deprotonation of the catalytic water molecule. Thus, it is reasonable to assume that the  $pK_a$  change of the  $\gamma$ -phosphate ( $\Delta pK_a^A$ ) will be larger than the corresponding change of the  $pK_a$  difference between the acceptor and donor ( $pK_a^A - pK_a^D$ ), and with this in mind, we can write  $\Delta \Delta G^{\ddagger} = \alpha \Delta pK_a^{AD} = \alpha \Delta pK_a^A - \alpha \Delta pK_a^D \approx \beta \Delta pK_a^A$ , where the correlation coefficient  $\beta$  (which is the one determined experimentally by correlating the reaction rate with the  $pK_a$  of the  $\gamma$ -phosphate) is smaller than  $\alpha$  since  $\Delta pK_a^D$  is likely to have the same sign as  $\Delta pK_a^A$ . Assuming that the linear correlation is maintained (which seems to be supported by the experimentally observed LFER), we conclude that the experimentally observed LFER with  $\beta = 2.1$  corresponds to an  $\alpha$  value of at least 2.1. This means that if we could measure the change of  $\Delta pK_a^{AD}$  we would have found that the corresponding change in  $\log(k_{cat})$  is at least twice as large. Throughout this paper, we will always refer to the experimentally observed LFER coefficient  $\beta$  rather to the more rigorous parameter  $\alpha$ . However, our conclusions about the mechanistic implications of the observed LFER are not likely to change with discussion of  $\beta$  instead  $\alpha$ .

that the LFER for the special case of electron transfer reactions can be obtained from the intersection of two parabolas that describe the free energies of the reactant and product states. This important result was based, however, on the assumption that the solvent can be represented by a dielectric continuum. Before considering microscopic justifications of using parabolas to describe chemical reactions, we try to explain in a simple qualitative way the LFER obtained by the use of parabolic free energy functions. Let us assume that the simple proton transfer reaction can be described by representing the reactant and product by two valence bond (VB) resonance structures, where the bonds are either fully made or broken and groups are either neutral or fully ionized. In this case it is possible to describe the reaction free energy in the way depicted schematically in Figure 2a. In this description, we obtain the potential surface of the reaction under study by mixing the two individual free energy functions  $g_I$  and  $g_{II}$  of the pure reactant and product states which are described by parabolic functions. The intersection of the two free energy parabolas determines the position of the transition state on the corresponding reaction coordinate. When the relative energy of the reactant and product state changes, the energy of the transition state changes, and this leads to a LFER of the type assumed by eq 8 (see Figure 2b).

To better understand the use of the free energy diagrams, it is useful to consider a simple case where a change in the reaction environment solely affects the energy of state II, for example, the mutation of a dipole that stabilizes state II. Such a perturbation will lead to an increase in energy of this state and will therefore shift the corresponding parabola up without changing its position relative to the reaction coordinate [see Warshel et al. (1994) for a detailed discussion of this procedure]. It is obvious from the schematic description of Figure 2a that this not only will change the equilibrium free energy,  $\Delta G^\circ$ , and thus, the  $\Delta pK_a^{\text{AB}}$  of the PT step but also will increase the free energy of activation,  $\Delta G^\ddagger$ , by raising the highest point in the reaction energy diagram, the transition state of this reaction. From the schematic description presented in panels a and b of Figure 2, one can see that a LFER is obtained as a direct result of the assumption that the free energy functions are parabolas. The validity of this approximation in realistic microscopic systems has been established by simulation studies [e.g., Hwang and Warshel (1987), King and Warshel (1989), and Charhaski et al. (1988)] and was found to be valid even in enzyme active sites where it is hard to accept a continuum dielectric description (Warshel et al., 1990; Yadav et al., 1991; Åqvist et al., 1994).

When the free energy profile is described by parabolas, it is possible to determine the position of the transition state by simple geometric algebra of intersecting parabolas. In the case of electron transfer reactions, one obtains the well-known Marcus relationship [e.g., Marcus (1964)]. Although this relationship has been used extensively in studies of general chemical reactions and is now also being used in studies of enzymatic reactions [e.g., Gerlt and Gasmann (1993), Guthrie and Kluger (1993), and Ren et al. (1995)], it is not fully valid in cases of adiabatic reactions where the relevant states interact strongly.<sup>4</sup> In such cases, one should consider the free energy function of different valence bond intermediates and take into account the coupling between these states. This leads to a modified Marcus relationship of Warshel and co-workers [see e.g. Hwang et al. (1988), Åqvist and Warshel (1993), Warshel (1991), and Warshel et al. (1994)]:

$$\Delta G^\ddagger \approx \frac{(\lambda + \Delta G^\circ)^2}{4\lambda} - H_{12} + \frac{H_{12}^2}{\lambda + \Delta G^\circ} \quad (9)$$

where  $\lambda$  is the so-called reorganization energy that is defined in Figure 2 while  $H_{12}$  is the term that describes the resonance mixing of the two interacting states (see Figure 2a). Note that eq 9 without the  $H_{12}$  and the  $H_{12}^2/(\lambda + \Delta G^\circ)$  terms is identical to the Marcus equation (Marcus, 1964). The differentiation of eq 9 yields now

$$\frac{\Delta \Delta G^\ddagger}{\Delta \Delta G^\circ} \approx \frac{\lambda + \Delta G^\circ}{2\lambda} \approx \frac{1}{2} + \frac{\Delta G^\circ}{2\lambda} \quad (10)$$

$$\Delta \Delta G^\ddagger \approx \left(\frac{1}{2} + \frac{\Delta G^\circ}{2\lambda}\right) \Delta \Delta G^\circ = \beta \Delta \Delta G^\circ \quad (11)$$

where we neglected the  $H_{12}^2$  term. Thus, eq 9 leads to a LFER of the type considered in eq 8. Note that  $\beta$  is constant only for small changes in  $\Delta G^\circ$  (eq 11). In adiabatic chemical reaction, that can be described by just two states, and in the range  $\lambda \geq \Delta G^\circ$ , one obtains a LFER coefficient  $\beta$  smaller than 1 [see also Warshel (1991)]. Observation as well as

prediction of LFER with a  $\beta$  of  $\leq 1$  is not new. What is quite different, however, is the deterministic feature of eq 11 that relates  $\beta$  in a unique way to the number of assumed states and their energies.<sup>5</sup> Thus, the VB approach leads to the conclusion that when  $\beta$  is larger than 1 the chemical reaction must be represented more than two states (see below).

#### *Probing the Free Energy Surface of the Intrinsic GTPase Reaction*

Many chemical reactions that are catalyzed by enzymes are characterized by more than one single step and therefore cannot be described by just two free energy functions. For the GTPase mechanism proposed for p21<sup>ras</sup> (Schweins et al., 1994, 1995), one can assume for example a potential surface consisting of at least four states (Figure 1). Following the approach of the preceding section, we may try to represent these four VB resonance structures by parabolic energy functions as shown in the hypothetical energy diagram of Figures 3 and 4. The transition state for a reaction is determined by the intersection of the two free energy functions that are highest in energy (as for example the intersection of parabola I and II in Figure 3), and the mixing of the individual free energy function will lead to the actual free energy surface for the given multistep reaction under study.

With the assumed four-state model, we may examine different mechanistic options by drawing the corresponding parabolas and comparing the resulting LFER to the one observed experimentally (Figure 2 of the preceding paper). We start with the mechanism of Figure 3, which implies that the proton transfer from the water molecule to the phosphates (state I  $\rightarrow$  state II of Figure 3) determines the overall activation barrier for the GTPase reaction ( $\Delta G^\ddagger = \Delta G_{\text{I-II}}^\ddagger$ ). As is clear from the figure, the LFER of this hypothetical system corresponds to a two-state model (that correlates  $\Delta G_{\text{I-II}}^\ddagger$  with  $\Delta G_{\text{I-II}}^\circ$ ). Thus, as argued in the previous section, one should expect a correlation coefficient  $\beta$  that is between 0 and 1 for reasonable changes of the height of the parabola of state I relative to the parabola of state II

<sup>4</sup> Recent attempts to use Marcus' relationship in analysis of enzymatic reactions tried to evaluate the so-called "intrinsic barrier"  $\Delta G_{\text{int}}^\ddagger$  which corresponds to the activation barrier for  $\Delta G^\circ = 0$ . These studies gave  $\lambda$  values which are significantly smaller than those obtained by realistic simulations. This discrepancy is due to the fact that the  $H_{12}$  term of eq 9 does not appear in the Marcus formula. That is, the correct  $\Delta G_{\text{int}}^\ddagger$  should be given by  $\lambda/4 - H_{12} + H_{12}^2/(\lambda + \Delta G_0)$ , and the  $\lambda$  deduced from this expression is very different than that obtained while neglecting  $H_{12}$  [see Kong and Warshel (1995)].

<sup>5</sup> The traditional LFERs are basically empirical relationships that classify reactions according to the observed LFER, rather than predict the LFER expected for the given assumed mechanism. On the other hand, eq 9 is much more deterministic since its validity has been proven rather than assumed by first principle microscopic simulations [e.g., Hwang et al. (1988)]. With eq 9 and the resulting eq 11, one concludes that any system that can be described by two VB states must have  $\beta = 0.5$  for  $\Delta G^\circ = 0$ . Thus, when  $\beta \neq 0.5$  for  $\Delta G^\circ = 0$ , we must have more than two states [e.g. see Warshel et al. (1994)]. The observation of very large  $\beta$  can be explained in a natural way by a three-state model and is hard to rationalize by traditional empirical LFER approaches. The VB description allows one to ask mechanistic questions in a quantitative way and to establish a clear relationship between the actual energies of intermediate states and the effect of different mutations. This point is best demonstrated in the discussion of Figure 7, where we use assumed VB charges and assume a charge shift of the protein to examine the corresponding  $\beta$ . We are not aware of any such predictive option with traditional empirical LFERs.

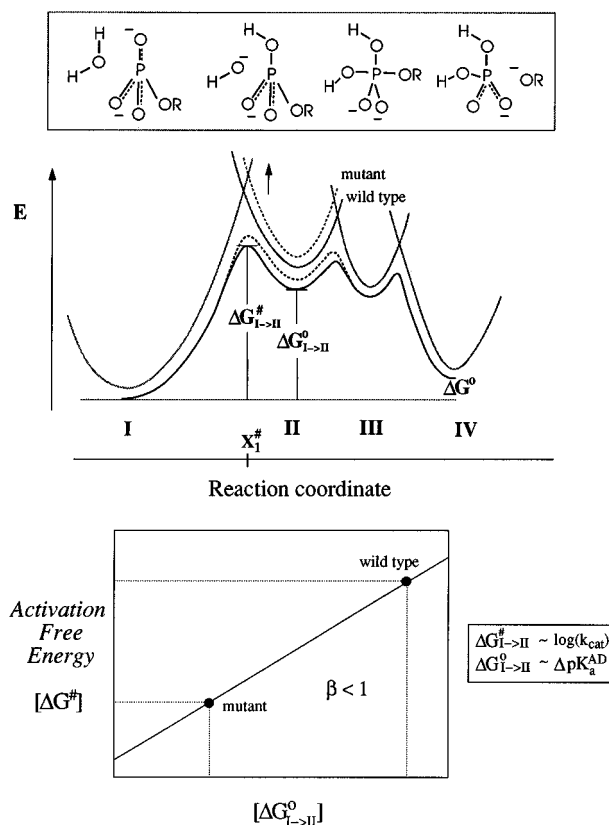


FIGURE 3: Hypothetical energy diagram in which the first step (the PT step) represents the transition state of the reaction. This diagram also exhibits a LFER correlation between  $\Delta G^\ddagger$  [ $\log(k_{cat})$ ] and  $\Delta G^0$  ( $pK_a$ ). The corresponding Brønsted plot (lower part of this figure) illustrates that the Brønsted slope  $\beta$  would be smaller than 1. Shifting state III or state IV would change neither  $\Delta G_{I \rightarrow II}^\ddagger$  [ $\log(k_{cat})$ ] nor  $\Delta G_{I \rightarrow II}^0$  ( $pK_a$ ). This reaction is comparable to a simple two-state model as presented in Figure 2. Thus, for a reaction where the first step is rate-determining, one would expect a Brønsted slope  $\beta$  smaller than 1. Since the experimentally observed correlation coefficient is  $\beta = 2.1$ , we conclude that the model profile presented in this figure does not represent the situation in  $p21^{ras}$ .

(see the LFER diagram in the lower part of Figure 3). This means that the model of Figure 3 in which the actual transition state of the reaction is part of the PT step is inconsistent with the observed LFER in  $p21^{ras}$  ( $\beta = 2.1$ ). However, as is pointed out below, this does not mean that the PT step cannot contribute to the overall barrier.

Other mechanistic options are examined in Figures 4 and 5. In these cases, the transition state is part of the nucleophilic attack. Mutations that only affect the energy of state II lead to a  $\beta$  of  $\leq 1$  (Figure 4), which is inconsistent with the observed LFER. In order to account for the observed Brønsted slope ( $\beta > 1$ ), it is essential that the change in activation energy involve state III and/or state IV. For example, the extreme case of  $\beta \gg 1$  occurs when a mutation only changes state III while leaving state II unchanged (illustrated in Figure 5). In fact, such large values for  $\beta$  were found for some mutants of tyrosyl-tRNA synthetase (Fersht et al., 1986) as well as for some Ras mutants (Figure 3 of the preceding paper). The corresponding analysis suggests that the oncogenic Ras mutant Q61L destabilizes exclusively the pentacoordinate phosphate (state III), while it does not affect state I or state II. The exact value of  $\beta = 2.1$  can be rationalized in models that involve changes in state III and/or state IV as well as state II. The question is, however, which of these models is consistent

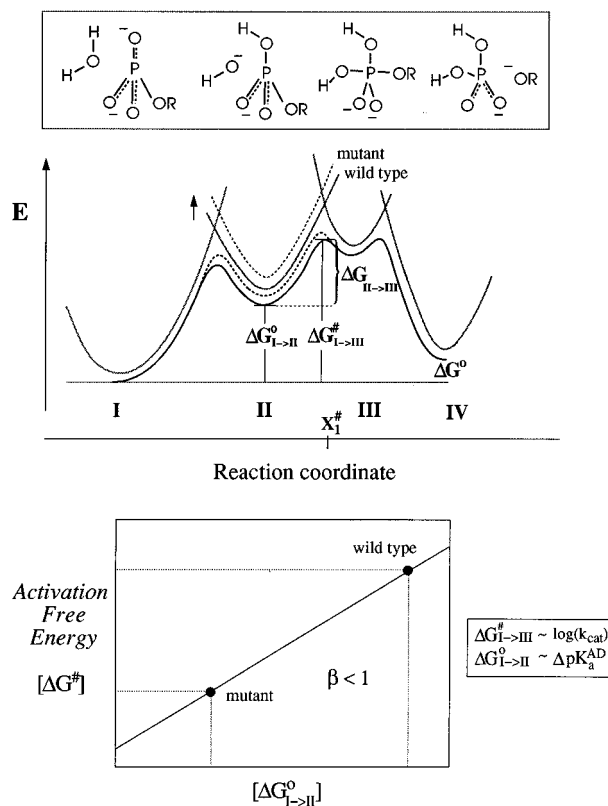


FIGURE 4: Schematic description of the relationship between the free energy difference,  $\Delta G^0$ , and the activation energy in a four-state model that describes different feasible limits in the reaction of  $p21^{ras}$ . In the upper part of this figure, a model is presented in which the second step of the reaction (the nucleophilic attack of the  $OH^-$  ion) occurs at the highest TS. A mutant that exclusively destabilizes state II would change at the same time the activation energy,  $\Delta G_{I \rightarrow II}^\ddagger$  (which is determined by the overall rate of the reaction  $k_{cat}$ ), and the equilibrium free energy,  $\Delta G_{I \rightarrow II}^0$  (the  $pK_a$  of the initial proton transfer). This model leads to  $\beta \leq 1$ . The lower part of this figure shows the corresponding Brønsted plot. Note that any mutation that destabilizes state II would display a Brønsted slope  $\beta$  of less than 1. The same is true if the energy of state II is changed and at the same time also the energy of state I. However, as soon as energy changes of state III are included, the corresponding Brønsted slope  $\beta$  might change to values larger than 1 (see Figure 5 for example). The fourth state as presented in this diagram is not identical with the product of the reaction, since the phosphate is still bound to the active site, while in the actual product, only GDP is bound to  $p21^{ras}$ . Models where state IV intersects with state II near the intersection with state III can also lead to a  $\beta$  of about 2.

with the structure of the active site, the assumed mechanism, as well as the nature of the relevant mutations. The VB description allows us to explore this by correlating a changing charge distribution within the active site with free energy changes of the relevant VB states (whose charge distributions are known to a reasonable approximation). A very qualitative model that accounts for the observed LFER is considered in a subsequent section. A more systematic analysis is left to subsequent studies.

The above LFER analysis indicates that the PT step is completed (or almost completed) at the transition state of the GTPase reaction catalyzed by Ras (if this reaction can be described by the above four-state model). Another way to verify this conclusion is the use of isotope effects [for review, see Schowen and Schowen (1982) and Cleland (1990)]. For many enzyme-catalyzed reactions, solvent isotope effects  $k_{H_2O}/k_{D_2O}$  of two or more are observed when the transition state involves a PT step (Fersht, 1984). Thus,

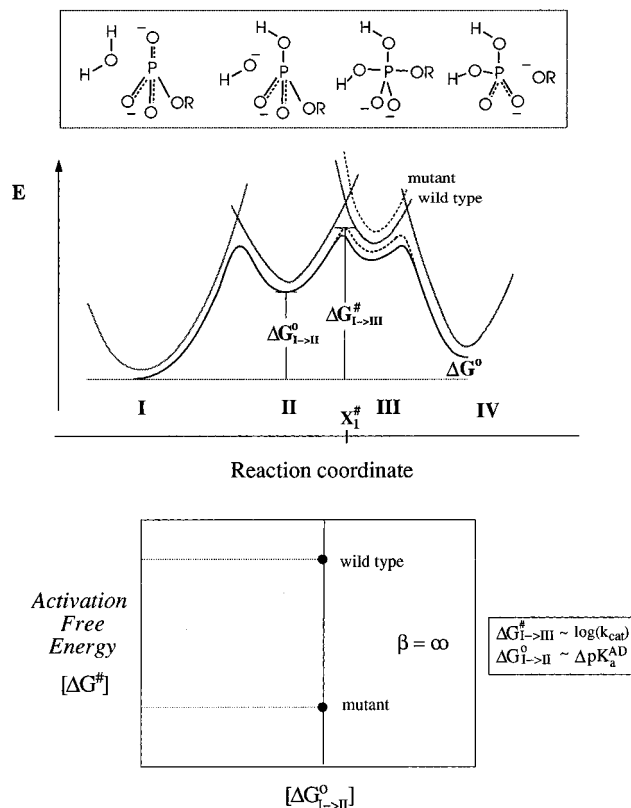


FIGURE 5: Same model profile as in Figure 4 illustrating how a mutant that exclusively destabilizes state III would change the activation energy  $\Delta G_{I \rightarrow III}^\ddagger$  without having an influence on the corresponding equilibrium free energy  $\Delta G_{I \rightarrow II}^\circ$ . This scenario leads to a correlation coefficient that can be as big as infinity. In fact, the Ras mutants Q61L and G12D exhibit a Brønsted slope  $\beta$  of  $\gg 1$ .

the exchange of the catalytic active water molecule by  $D_2O$  and determination of a resulting change in reaction rate should help to clarify if the PT from Wat175 to the  $\gamma$ -phosphate in p21<sup>ras</sup> represents the overall transition state of the reaction. In Table 1, we compare the catalytic properties of wild type Ras in  $H_2O$  and in  $D_2O$ . It can be seen from these data that the intrinsic reaction is not slowed in the presence of  $D_2O$ . In fact, the GTPase reaction in  $D_2O$  is even slightly faster than the corresponding reaction in conventional  $H_2O$ . Thus, this result also supports the proposal that the initiating PT step of the reaction catalyzed by p21<sup>ras</sup> does not include the transition state.

Solvent isotope effects can be caused not only by direct PT in the transition state of the rate-limiting step but also as a result of perturbation of a pre-transition-state equilibrium. Thus, the fact that the reaction in  $D_2O$  is even slightly faster than that in  $H_2O$  might for example be due to a  $pK_a$  increase of Ras-bound GTP in  $D_2O$ . The Brønsted type LFER found for p21<sup>ras</sup> suggests that any effect that will change the  $pK_a$  of the terminal phosphate group of GTP should also accelerate the reaction rate. In fact, from studies with phosphoric acid, it is known that the corresponding  $pK_a$  in  $D_2O$  is slightly higher than that in conventional  $H_2O$  (Jencks & Salvesen, 1971). The effect of pre-transition-state equilibria on the rate of the GTPase reaction is addressed in the next section. The observed inverse solvent isotope effect might also be due to secondary isotope effects or to the exchange of some protons with deuterons that are either

Table 1

	intrinsic GTPase		GAP-catalyzed GTPase		
	$k_{cat}$ ( $\text{min}^{-1}$ )	$k_{cat}$ ( $\text{s}^{-1}$ )	$K_m$ (mM)	$k_{cat}/K_m$ ( $\text{mM}^{-1} \text{s}^{-1}$ )	
p21-Mg <sup>2+</sup> $H_2O$	0.028	19.1	8.9	2.1	
p21-Mg <sup>2+</sup> $D_2O$	0.038	26.2	12.7	2.1	
p21-Mg <sup>2+</sup> $k_{H_2O}/k_{D_2O}$	0.732	0.75	0.71	1.00	

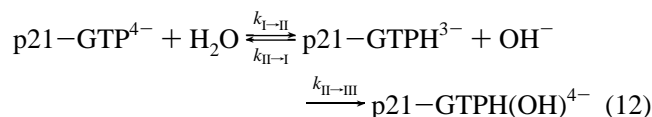
directly or indirectly involved in the stabilization of the transition-state structure.

The theoretical analysis that led to the GTP as a base proposal (Schweins et al., 1994) also suggests that the  $OH^-$  attack on the  $\gamma$ -phosphate and not the initial PT step occurs at the highest TS. In this study, different alternative reaction mechanisms were tested, and only the GTP as a base mechanism was found to be consistent with the observed activation barriers of the intrinsic reaction. The calculation considered an initial PT step before the  $OH^-$  nucleophile attacks.

#### Pre-Transition-State PT Steps Can Contribute to the Overall Activation Barrier

From the definition of general base catalysis, it is obvious that the stronger the general base, the faster the corresponding reaction rate. As the preceding section shows, there is strong evidence that the initial PT step does not involve the overall transition state of the Ras-catalyzed GTPase reaction. A superficial analysis might lead to the conclusion that the PT step is not rate-determining and therefore should not be considered in analyzing the energetics of the reaction. Yet, the observed LFER between the logarithm of the GTPase rate and the  $pK_a$  of protein-bound GTP demonstrates that this step indeed has an effect on the overall reaction rate. Thus, it is important to understand how the equilibrium free energy (and thus the  $pK_a$  difference between the proton acceptor and the proton donor) of a PT step that precedes the actual transition state might influence the overall reaction rate of a chemical reaction in general.

Even though the PT step is very likely not the “kinetic bottleneck” for the reaction, it still can have an effect on the overall GTPase rate. In order to illustrate this point, it is helpful to assume for the proposed GTPase reaction mechanism a kinetic scheme of the form



where the nucleophilic attack of the  $OH^-$  is supposed to be rate-determining. Since for the GTP as a base mechanism of p21<sup>ras</sup> the equilibrium of the PT is on the reactant side, we can assume that  $k_{I \rightarrow II} < k_{II \rightarrow I}$  and it follows

$$\begin{aligned} \text{rate}_{I \rightarrow III} &= k_{cat}[p21-GTP^{4-}][H_2O] \\ &= k_{II \rightarrow III}[p21-GTPH^{3-}][OH^-] \\ &\approx k_{II \rightarrow III} \left( \frac{k_{I \rightarrow II}}{k_{II \rightarrow I}} \right) [p21-GTP^{4-}][H_2O] \end{aligned} \quad (13)$$

and with the help of transition-state theory one obtains

$$\text{rate}_{\text{I} \rightarrow \text{III}} \approx \left( \frac{k_B T}{h} \right) \exp \left[ - \left( \frac{\Delta G_{\text{I} \rightarrow \text{II}}^\circ + \Delta G_{\text{II} \rightarrow \text{III}}^\#}{k_B T} \right) \right] \times \quad (14)$$

$$[\text{p21-GTP}^{4-}][\text{H}_2\text{O}] = \left( \frac{k_B T}{h} \right) \exp \left[ - \left( \frac{\Delta G_{\text{I} \rightarrow \text{III}}^\#}{k_B T} \right) \right] \times$$

$$[\text{p21-GTP}^{4-}][\text{H}_2\text{O}]$$

where  $k_B$  is the Boltzmann constant,  $T$  the absolute temperature, and  $h$  Planck's constant. Although we assumed a quasi-equilibrium for the first step, the same result would be obtained with more rigorous treatments as long as  $\Delta G_{\text{I} \rightarrow \text{II}}^\circ > 0$  and  $\Delta G_{\text{I} \rightarrow \text{III}}^\# > \Delta G_{\text{I} \rightarrow \text{II}}^\#$ . The highest energy barrier in the proposed free energy surface for GTP hydrolysis in p21<sup>ras</sup> corresponds to  $\Delta G_{\text{I} \rightarrow \text{III}}^\#$  (Figure 4). In order to reach this level, the system must first get to the level of  $\Delta G_{\text{I} \rightarrow \text{II}}^\circ$  and then acquire an additional energy,  $\Delta G_{\text{II} \rightarrow \text{III}}^\#$ . Thus, from this as well as from eq 14, one can conclude that the overall activation barrier of the system,  $\Delta G_{\text{I} \rightarrow \text{III}}^\#$  that determines  $k_{\text{cat}}$  is given to very good approximation by the sum of  $\Delta G_{\text{I} \rightarrow \text{II}}^\circ$  and  $\Delta G_{\text{II} \rightarrow \text{III}}^\#$ . Any increase in the equilibrium free energy of the PT step from water to GTP,  $\Delta G_{\text{I} \rightarrow \text{II}}^\circ$ , will affect the activation barrier of the reaction,  $\Delta G_{\text{I} \rightarrow \text{III}}^\#$ , even though it is just a preceding equilibrium that is not part of the highest transition state of the reaction. From this derivation, it is clear that any pre-transition-state equilibrium including conformational changes of the protein might have an influence on the reaction rate of an enzyme. For the GTPase reaction catalyzed by p21<sup>ras</sup>, we can conclude that the nucleophilic step of the OH<sup>-</sup> ion represents the kinetic bottleneck (since it passes through the configuration with the lowest probability), while the preceding PT step can be described as the thermodynamic bottleneck of this reaction.

#### *Gln as a Proton Shuttle and Other Alternative Mechanisms*

Since the guanine nucleotide binding proteins share common highly conserved sequence motifs and are also closely structurally related, it is reasonable to assume that this structural homology is followed by functional homology. Thus, p21<sup>ras</sup>, EF-Tu, transducin- $\alpha$ , and other GTP-binding proteins of the enormous superfamily are very likely to share the same reaction mechanism, with small deviations that explain the different reaction rates.

Recently, an appealing alternative GTPase mechanism was proposed on the basis of a high-resolution X-ray structure of the Ras-related transducin- $\alpha$  complexed with GDP-AlF<sub>4</sub><sup>-</sup> (Sondek et al., 1994). In this proposal, water attacks the  $\gamma$ -phosphate in a concerted fashion, while a proton is being abstracted by the Gln61 side chain, which simultaneously protonates an oxygen of the  $\gamma$ -phosphate. This leads to the formation of the unfavorable tautomeric form of the glutamine side chain and the pentacoordinate  $\gamma$ -phosphate reaction intermediate (Figure 6). Since in this reaction scheme the  $\gamma$ -phosphate group of GTP is also the final proton acceptor, the concerted Gln proton shuttle mechanism can be viewed as an extension of the GTP as a base mechanism, where a Gln side chain is directly involved in the bond making and bond breaking processes (Figure 6). However, while in the GTP as a base mechanism the PT step and the nucleophilic attack occur sequentially the concerted Gln proton shuttle mechanism is characterized by bond-making and -breaking

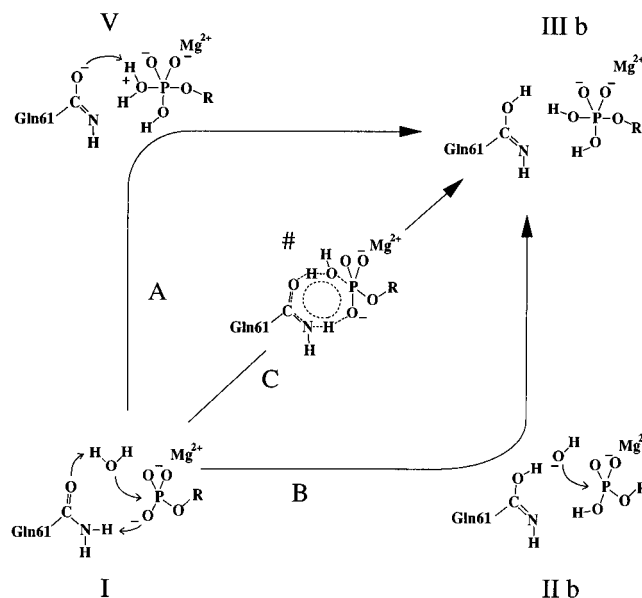


FIGURE 6: Rectangular free energy diagram of the concerted Gln as a proton shuttle mechanism. The reaction sequence C represents the concerted Gln61 proton shuttle mechanism as proposed by Sigler and co-workers (Sondek et al., 1994). The notation of the different states (I, IIb, and IIIb) follows the numbering of Figure 1 (I, II, and III), while # denotes the proposed transition state in a hypothetical Gln61 proton shuttle mechanism. The subscript b indicates that the energy of the corresponding states of the Gln as a proton shuttle mechanism (IIIb) is identical to that of the corresponding states of the GTP as a base mechanism (III), with the exception of the amide side chain of the Gln that is left in its energetically unfavorable "enol" configuration ( $\Delta G_{\text{(keto} \rightarrow \text{enol)}} \approx 16$  kcal/mol). Since in this reaction scheme the  $\gamma$ -phosphate group of GTP is also the final proton acceptor, the concerted Gln as a proton shuttle mechanism can be viewed as an extension of the GTP as a base mechanism, where a Gln side chain is directly involved in the bond-making and bond-breaking processes. Note that the transition state (#) is formed by a ring of eight atoms that are donated by three residues (Gln61, Wat, and  $\gamma$ -phosphate). To examine the validity of a proposed mechanism, it is necessary to relate the assumed chemistry to the relevant energetics. While a typical stepwise mechanism (A and B) proceeds along the edges of these diagrams, the concerted path is characterized by passing through the center region of the diagram (C). Very often, it is possible to analyze the energetics of the concerted mechanism once the corners of the energy diagram are determined. The text explains why the Gln proton shuttle mechanism is always unfavorable relative to the GTP as a base mechanism.

processes that happen simultaneously. The notation in Figures 1 and 6 was chosen to indicate the close relationship between these two mechanisms.

It is always necessary to relate the assumed chemistry to the relevant energetics in order to find out if a proposed reaction mechanism is operative in a given enzyme. Many concerted mechanisms can be described in terms of rectangular free energy diagrams, whose corners correspond to well-defined resonance structures with different bonding arrangements and where bonds are either fully made or broken and charges fully localized on ionized fragments (Warshel, 1991). Such diagrams have been used frequently in the past to describe chemical and biological reactions in a qualitative way without considering the actual energies of the reactants, intermediates, and products [e.g. Davis et al. (1988)]. However, the power of such approaches is augmented tremendously when energies of the resonance structures that span the corners of these systems are available from the relevant experimental and theoretical information (Warshel & Weiss, 1980; Pross & Shaik, 1983). This helps

us find the actual reaction path and better understand the nature of a concerted mechanism.

In order to analyze the energetics of the concerted mechanism, we have to examine the relevant rectangular free energy diagram (Figure 6). The corresponding stepwise mechanism proceeds along to the edges of the diagram (A and B in Figure 6), while the concerted path is characterized by passing through the center region of the diagram (C in Figure 6). In many cases, it is possible to analyze the energetics of the concerted mechanism once the corners of the energy diagram of the relevant reference reaction in water are determined (Warshel, 1991). In fact, the energy of a concerted path is strongly correlated with the energy of the corresponding nonconcerted paths. From Figure 6, it can be seen that the concerted Gln proton shuttle mechanism (route C) is defined by the transition from the reactant state (I) to the pentacovalent intermediate (III<sub>b</sub>). The edges of this diagram consist of stepwise reaction routes (route A and route B). As shown below, this diagram leads to the conclusion that the Gln proton shuttle mechanism is always unfavorable relative to the GTP as a base mechanism. That is, the pentacovalent intermediate state of the Gln as a proton shuttle mechanism (III<sub>b</sub> in Figure 6) is identical to the corresponding state of the GTP as a base mechanism (III in Figure 1), with the exception of the amide side chain of the Gln that is left in its energetically unfavorable "enol" configuration. Thus, for the energy of the pentacovalent intermediate, we obtain

$$\Delta G_{\text{III}_b} = \Delta G_{\text{III}} + \Delta G_{(\text{keto} \rightarrow \text{enol})} \quad (15)$$

Very recently, the energetics of the tautomerization of formamide, including solvent effects, were analyzed by several high-level *ab initio* approaches (Hroudá et al., 1994; Adamo & Lelj, 1995). From these results, it can be concluded that the equilibrium free energy,  $\Delta G_{(\text{keto} \rightarrow \text{enol})}$ , between the amide and the amidinic acid in aqueous solution is at least 16 kcal/mol. Since the equilibrium free energy of state III,  $\Delta G_{\text{III}}$ , in aqueous solution is around 34 kcal/mol (Schweins et al., 1994), the energy of the pentacoordinated intermediate of the Gln as a proton shuttle mechanism (III<sub>b</sub>) is in water at least 50 kcal/mol. The corresponding activation barrier,  $\Delta G^\ddagger$ , is expected to be even higher than this. Our energy consideration suggests that the formation of an enolic reaction intermediate in the active site of an enzyme is also highly unfavorable and therefore not very likely. Note that the reaction routes A and B in Figure 6 also contain steps (as for example the attack of a neutral water molecule or the protonation of Gln) that are energetically disadvantageous. In fact, because of the very low  $\text{pK}_a$  of the amide group, a proton transfer to Gln61 can be excluded for any mechanism that is discussed for the GTPase of p21<sup>ras</sup> (Langen et al., 1994; Schweins et al., 1995). The nucleophilic attack of a neutral water molecule was shown before to be energetically unfavorable (Schweins et al., 1994).

Another fact that is inconsistent with the Gln61 as a proton shuttle mechanism is the observed isotope effect. That is, since the nucleophilic attack occurs at the same time as the proton transfer step, one would assume for this mechanism that the proton transfer is part of the transition state and hence also part of the rate-limiting step. Thus, one would expect for instance a large solvent isotope effect. However, the results presented in this work contradict this prerequisite.

One might still argue that the resonance interaction in the transition state of the concerted mechanism may contribute significantly to a reduction in activation free energy,  $\Delta G^\ddagger$ . In general, for a true concerted reaction, all atoms that participate in bond breaking and making are required to be in a highly ordered state. However, having eight transition-state atoms with their orbitals in the right orientation is not only sterically very demanding but also entropically extremely expensive. This is especially true for the proposed concerted Gln proton shuttle mechanism since the reactants (Gln61, Wat165, and the  $\gamma$ -phosphate) are not constrained relative to each other but rather can move relatively independently. Therefore, the system is characterized by many degrees of freedom. This makes a concerted reaction even more unlikely.

Regardless of how convincing the entropic and isotope effect arguments are, our strongest point is clearly the energy-based analysis given above, which shows that the energy in point III<sub>b</sub> is uniquely given by eq 15 (regardless of the pathway that leads from I to III<sub>b</sub>), and the entire mechanistic issue boils down to the value of  $\Delta G_{(\text{keto} \rightarrow \text{enol})}$ .

In the examination of different mechanistic options, it is interesting to consider a recent proposal for the mechanism of ATP hydrolysis in myosin (Fisher et al., 1995). This proposal also considers the  $\gamma$ -phosphate as the base but invokes Ser236 as a shuttle in the transfer of a proton from the catalytic water to the  $\gamma$ -phosphate. It has been argued that the involvement of Ser236 provides a better stereochemistry for the PT step than the direct PT process (Fisher et al., 1995). Note that the Ser236 as a shuttle mechanism also operates with GTP as the final base and thus is closely related to the GTP as a base mechanism which includes a direct PT step. Our experience with EVB simulations suggests that moving the catalytic water for an optimal PT process does not cost more than 1–2 kcal/mol, while the entropic penalties of using intermediates can be significant. Resolving this issue would require computer simulations and additional mutational studies. It is obvious that the highly conserved amino acid Ser236 in myosin is important. However, Ser236 might play a special role in stabilizing the transition state without being directly involved in the actual chemical processes of the hydrolysis reaction.

Another mechanism that should be considered for GTP and ATP hydrolysis catalyzed by enzymes is a specific acid/base mechanism where the  $\gamma$ -phosphate is protonated by a water molecule while a second neutral water molecule attacks the protonated  $\gamma$ -phosphate. However, even though this mechanism may account for the observed LFER, it still involves significant problems. That is, if the protonation involves a  $\text{H}_3\text{O}^+$  ion that comes from the bulk solvent, one should expect that  $k_{\text{cat}}$  would increase with decreasing pH [see discussion for the closely related case of the recently proposed specific base catalysis for DNA polymerase (Fothergill et al., 1996)]. However, the observed pH profile of the intrinsic GTPase reaction for Ras reveals that the corresponding rate is pH independent in the range pH 4–8 and decreases when the pH is lowered from 4 to 2 [Figure 3 in Schweins et al. (1995)]. This observation is more consistent with our GTP as a base mechanism than with the specific acid/base mechanism where the  $\gamma$ -phosphate is protonated by a  $\text{H}_3\text{O}^+$  ion that comes from the bulk solvent.

Although the experimentally observed pH profile is not in agreement with a specific acid/base mechanism where the  $\gamma$ -phosphate is protonated by a  $\text{H}_3\text{O}^+$  ion, it cannot be used



to exclude a related mechanism that involves two active site water molecules and in which one water molecule protonates the  $\gamma$ -phosphate while another attacks it. Preliminary energy considerations of the same type used in our previous study (Schweins et al., 1994) indicate that such a mechanism is less favorable than the GTP as a base mechanism. While the energies of the relevant reference reactions in water of these two mechanisms are similar, the active site of the protein stabilizes the doubly charged transition state of the GTP as a base reaction more than the corresponding singly charged transition state of the two-water mechanism. Nevertheless, more theoretical and experimental studies are needed before one can exclude (or accept) this mechanistic alternative.

A recent work of Maegley et al. (1996) made some interesting proposals that should be considered in our mechanistic discussion. This paper adopted our arguments against the Gln as a base mechanism but then suggested that the GTP as a base mechanism is "anticatalytic". This assertion has several major problems. First, it is implied that since the proton might be on the leaving group at the TS of the *dissociative* mechanism it should do the same in an *associative* mechanism. Thus, leaving the proton on the  $\gamma$ -phosphate at the transition state of the associative mechanism is anticatalytic. However, we are dealing here with two different mechanisms (associative and dissociative), and the proton can be located on different atoms in different mechanisms. Furthermore, the proton is a part of the reacting system and not a "catalyst". Second, although it is somewhat unclear as to what is the actual mechanism proposed by Maegley et al. (1996) (the attacking water is considered a leaving group rather than a nucleophile), if the proton is not transferred to the  $\gamma$ -phosphate at the TS, it is hard to see how the observed LFER can be accounted for.

Regardless of the above-mentioned problems, we cannot yet exclude a partially dissociative mechanism that involves the key of our GTP as a base mechanism (i.e. protonation of the  $\gamma$ -phosphate). However, the feasibility of the relevant mechanism cannot be deduced from solution experiments. That is, the only available energy-based analysis that compares the energetics of associative and dissociative mechanisms in aqueous solution indicates that these mechanisms have similar energetics in solution (Guthrie, 1977). This finding is supported by our recent *ab initio* studies (Florian & Warshel, in preparation). Since the energies of the associative and dissociative mechanisms in solution are similar, the question boils down to the effect of the electrostatic potential from the protein active site on the charge distribution of the relevant VB states in the associative and dissociative mechanisms. Such a study is now underway. It is important to point out in this respect on the suggestion that the small effect of  $\text{Mg}^{2+}$  ions on the phosphate hydrolysis reaction in aqueous solution supports dissociative mechanisms in proteins [e.g. Hollfelder and Herschlag (1995)]. This interpretation overlooks the fact that the dielectric constant in water drastically reduces electrostatic effects and that the situation is entirely different in active sites of proteins [see the discussion of a related charge stabilization effect in water and in lysozyme in Warshel (1991)]. Our studies of the electrostatic effects of metal ions on phosphate hydrolysis in proteins [e.g. Schweins et al. (1994) and Fothergill et al. (1995)] clearly indicate that these effects are very large.

### *Mechanism of GAP Activation of the p21<sup>ras</sup> GTPase Reaction*

While the intrinsic GTPase reaction seems to be responsible for the breakdown of the p21(GTP)–Raf kinase complex, the GTPase activating protein, GAP, down-regulates the amount of free activated p21(GTP) in the cell. Thus, understanding the intrinsic as well as the GAP-stimulated GTPase mechanism is of great importance for understanding signal transduction on an atomic level. On the other hand, it is of general interest to understand how a certain protein can effect the reaction rate of another enzyme.

In principle, two extreme classes of mechanism for GAP activation of the p21<sup>ras</sup> GTPase reaction are conceivable. In one of these, the basic mechanism is the same in p21<sup>ras</sup> and in the p21<sup>ras</sup>–GAP complex. In the other type of mechanism, the involvement of one or more side chains of the GAP molecule in the catalytic reaction is imaginable. So far, it has not been possible to observe any fundamental differences in chemistry between the intrinsic and the GAP-stimulated GTPase of p21<sup>ras</sup>.

This finding is also supported by the solvent isotope effect displayed in Table 1. As seen from these data, the intrinsic as well as the GAP-stimulated GTPase reaction in p21<sup>ras</sup> are in  $\text{D}_2\text{O}$  slightly faster than the comparable reaction in  $\text{H}_2\text{O}$ . From this result, it can be concluded that a proton transfer step is also not very likely to be the actual rate-determining step for the GAP-stimulated GTPase reaction of p21<sup>ras</sup>. The fact that the isotope effect,  $(k_{\text{H}_2\text{O}}/k_{\text{D}_2\text{O}})$  is very similar for the intrinsic and the GAP-stimulated reaction suggests that the chemistry of the intrinsic and the GAP-stimulated GTPase might also be similar.

In this context, it is very interesting to note that the correlation coefficient  $\beta$  for the GAP-catalyzed reaction is different from the corresponding coefficient for the intrinsic reaction. While the intrinsic reaction exhibits a Brønsted slope of  $\beta = 2.1$ , the corresponding value for the GAP-activated reaction is  $\beta = 4.9$  [see Schweins et al. (1996)]. A given  $\text{pK}_a$  change due to mutation seems to have a larger impact on the reaction rate when GAP is present.

The reason for the larger  $\beta$  for the GAP-bound p21<sup>ras</sup> cannot be determined uniquely without the X-ray structure of the GAP–p21<sup>ras</sup> complex. However, it is tempting to speculate on a possible explanation. That is, regardless of the exact mechanism of the GTPase reaction and the actual effect of the protein, we can describe the generic protein effect with Figure 7. As illustrated by the figure, the hydrolysis reaction in almost any conceivable mechanism involves a movement of a negative charge from the  $\gamma$ -phosphate to the  $\beta$ -phosphate. The protein can catalyze this charge shift process by rearranging its dipoles and charges in a way that is equivalent to the motion of a positive charge toward the  $\beta$ -phosphate (see Figure 7). Now the shift of this positive effective charge (whose possible origin will be discussed below) has several consequences. First, it is reasonable to assume that the effects of mutations will also result in a shift of the effective protein charge. The effect of this shift depends on the assumed mechanism, and our VB model allows one to examine this effect. For example, the hypothetical energetics and charges of Figure 7 predict that, when the reaction is accelerated by a given mutation, this mutation pushes the energies of states I, II, and III up and of state IV down. This will lead to correlated changes (since the same factors that reduce  $\Delta G_{\text{I} \rightarrow \text{II}}^\ddagger$  will also reduce

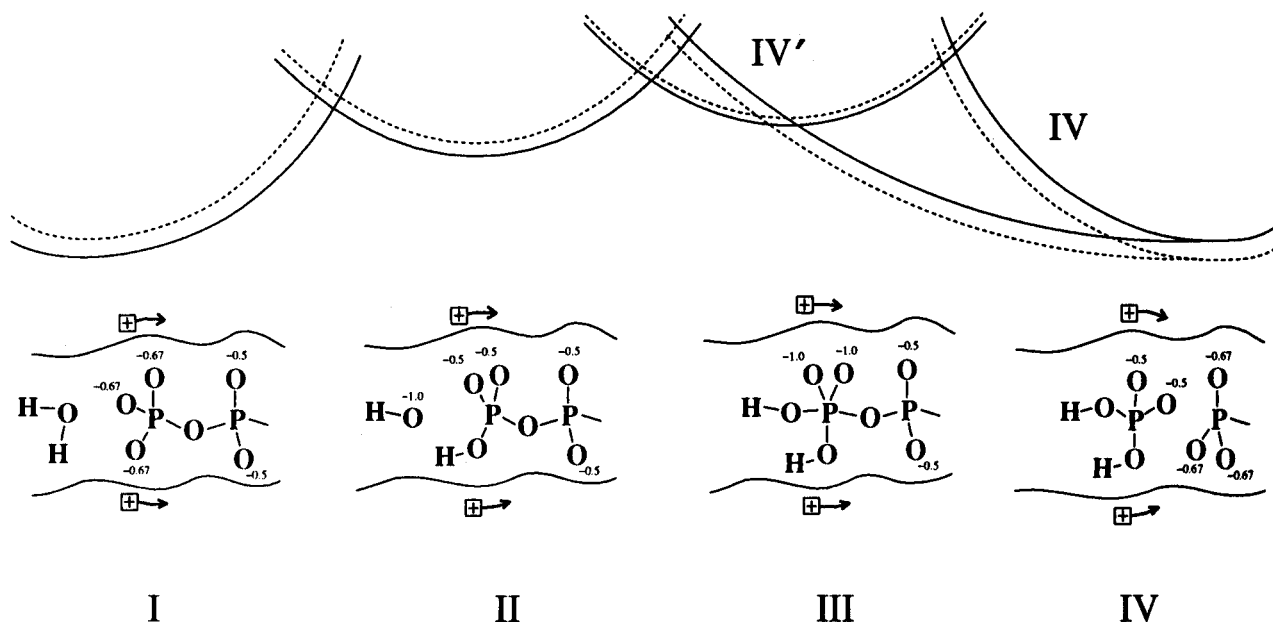


FIGURE 7: Energy diagram that can rationalize the observation of  $\beta > 1$  in  $p21^{\text{ras}}$ . This figure describes the effect of mutations in terms of a shift of an effective charge and the corresponding change of electrostatic interaction with the assumed four VB states. The activation barrier is determined by the intersection of state III and IV. In this specific case,  $\beta$  is approximately 4 as can be determined by measuring the relevant energy shifts from the figure and dividing  $\Delta G_{\text{I} \rightarrow \text{IV}}^{\ddagger}$  by  $\Delta G_{\text{I} \rightarrow \text{II}}^{\circ}$ . Another appealing possibility is that the TS occurs at the intersection of state II and state IV (the corresponding free energy curve of state IV is designated by IV'). The figure represents the hypothetical effect of mutations in the GAP-catalyzed reaction. As stated in the text, a smaller  $\beta$  for the intrinsic reaction can be rationalized by moving the effective protein charge further to the left.

$\Delta G_{\text{II} \rightarrow \text{III}}^{\circ}$ ) and can lead to a  $\beta$  of  $> 1$ . Second, if GAP moves the effective protein charge toward the  $\beta$ -phosphate, it will increase  $\beta$ , since now a mutation that results in a small additional shift of this charge will lead to a larger change of  $\Delta G_{\text{II} \rightarrow \text{III}}^{\circ}$  (and/or  $\Delta G_{\text{III} \rightarrow \text{IV}}^{\circ}$ ) and therefore to a larger  $\beta$ . The reader can examine this point by copying the parabolas of Figure 7 to transparencies and examining the effect of their shift on their highest intersection. Another appealing possibility involves the case where state IV intersects with state II near the intersection with state III. This associative  $S_N2$ -type mechanism will lead to a  $\beta$  of  $> 1$ .

With the above perspective, we can ask what mechanisms can lead to a shift of a positive effective charge. Muegge and co-workers (1996) proposed such a mechanism by pointing out that the transition of the protein from its GTP- to GDP-bound forms leads to a transfer of a positive potential from the  $\gamma$ -phosphate to the  $\beta$ -phosphate. If GAP pushes  $p21^{\text{ras}}$  toward its GDP-bound conformation, it will lead to a shift of effective positive charge and to rate acceleration as well as to a larger  $\beta$ .

Another somewhat equivalent possibility is associated with the proposal (Brownbridge et al., 1993; Mittal et al., 1996) that GAP provides a positively charged arginine side chain that directly interacts with the  $\gamma$ -phosphate and/or the bridging atom between the  $\beta$ - and  $\gamma$ -phosphate. This can result in a shift of the positive protein potential relative to that of the isolated  $p21^{\text{ras}}$ .

### Conclusion

The present work explores the basis for linear free energy relationships in chemical reactions, focusing on the observed effects of mutations in  $p21^{\text{ras}}$  and related systems. It is demonstrated that the LFER can be described and rationalized by using Marcus type parabolas that represent the reactant, intermediate, and product state of the reaction in a relevant energy diagram. It is illustrated that the correlation

between the activation free energy,  $\Delta G^{\ddagger}$ , and the equilibrium free energy,  $\Delta G^{\circ}$ , of a reaction is related in a simple way to the energy of the intersection of the corresponding energy states that are represented by parabolas. The only requirement for the description of the LFER by parabolas is that mutations will not change the curvatures of the actual parabolic free energy function.

In order to be able to explain the observed LFER in  $p21^{\text{ras}}$ , it is essential to describe the GTPase reaction in terms of more than two states. Such a model allows us to rationalize the observed Brønsted values of  $\beta = 2.1$  and  $\beta \gg 1$  for the two different classes of mutations. It is argued that as long as the active site does not change in a drastic way due to mutation and as long as the analyzed mutants exhibit a residual enzymatic activity the observation of a LFER implies that the reaction mechanism is unchanged despite small changes in the reaction conditions. Thus, one can use a LFER not only to study the reaction mechanism of a particular protein but also to examine whether certain mutants or even different proteins follow the same mechanistic reaction route.

The observed LFER for  $p21^{\text{ras}}$  is used to analyze the actual free energy surface and the corresponding reaction path of the intrinsic GTPase reaction. From this, a model reaction profile is constructed that explains how a LFER can arise and also how the different observed Brønsted coefficients can be rationalized. Our analysis indicates that the PT step does not occur at the transition state of the reaction. This conclusion is supported by solvent isotope effect studies. Nevertheless, it is illustrated that the overall activation barrier reflects the energy of the PT step, although this step does not occur at the highest TS.

An alternative mechanism similar to the GTP as a base mechanism was proposed recently for  $p21^{\text{ras}}$  and other GTP-binding proteins on the basis of a high-resolution structure of transducin- $\alpha$ . In this proposal, water attacks the  $\gamma$ -phos-

phate in a concerted fashion, while a proton is being abstracted by the Gln61 side chain, which in turn protonates an oxygen of the  $\gamma$ -phosphate. However, the simple energy consideration presented in this work demonstrates in a unique way that the mechanism that involves Gln61 has a significantly higher activation barrier compared to the GTP as a base mechanism (this was shown for the reference reaction in water, but a similar conclusion is expected for this system when the enzyme's active site is the solvent).

Other alternative mechanisms are also considered in this paper. This includes specific acid/base catalysis and a partially dissociative mechanism. In order for these mechanisms to be consistent with the observed LFER, they probably have to involve a PT to the  $\gamma$ -phosphate, thus reflecting a major element of the GTP as a base mechanism. Both mechanistic options are still feasible. We also find that an associative/ $S_N2$ -type version of our GTP as a base mechanism can account for the observed LFER. However, only energy-based analysis of all possible alternatives will eventually allow for determination of the exact mechanism of GTP and ATP hydrolysis. In this respect, progress toward a more unique identification of the transition state of the GTPase reaction in p21<sup>ras</sup> may require (i) a systematic *ab initio* analysis of phosphate hydrolysis in solution (with verification using experimental observations), (ii) EVB studies that transform the energies and charge distribution of different assumed mechanisms from solution to the enzyme active site, and (iii) calculation of the LFER for each of the feasible mechanisms and comparison with the experimentally observed LFER.

The result of more quantitative analysis can benefit from the recently available structures of transition-state analogs (Sondek et al., 1994). Although such structures cannot be used to directly deduce the reaction mechanism and perhaps not even to provide an exact representation of the real transition state, they provide major information about the relevant stereochemistry and about the reorganization of the protein environment that takes place during the reaction. These results not only strongly support the principle that GTP hydrolysis is an in-line attack of water probably in an associative manner (Eccleston & Webb, 1982; Feuerstein et al., 1989) but also help us to understand how catalysis via stabilizing interactions with the intermediate and structurally related transition states occurs (Goody, 1994). The structures of the proteins with bound transition-state analogs might eventually also tell us why some GTP binding proteins exhibit a slow GTPase rate and others a fast one even though these proteins share not only very similar ground-state structures but probably also the same reaction mechanism.

The analysis presented in this work indicates that the mechanism of GTP hydrolysis by GAP-activated p21<sup>ras</sup> seems to be closely related to that in p21<sup>ras</sup> alone. Up to this point, it has not been possible to observe any fundamental differences in chemistry between these systems. All perturbations that lead to a different intrinsic rate also lead to a comparable change of the GAP-stimulated reaction rate. This indicates that the GAP-stimulated reaction might also follow the GTP as a base mechanism. The role of GAP in the activation of the GTPase reaction could be the stabilization of the GDP-bound conformation in the active site of p21<sup>ras</sup> (Muegge et al., 1996). GAP might also lead to a change of electrostatic properties in the active site of p21<sup>ras</sup> since the active site of p21<sup>ras</sup> is directly located at the protein surface.

## Methods

**Protein Purification.** p21<sup>ras</sup> proteins and GAP proteins were purified as described in the preceding paper.

**Solvent Isotope Effect.** In order to determine the solvent isotope effect for the intrinsic as well as the GAP-stimulated GTPase reaction, we lyophilized p21–GTP and added D<sub>2</sub>O subsequently. To increase the D<sub>2</sub>O/H<sub>2</sub>O ratio, this procedure was repeated up to three times. The GTPase rates in D<sub>2</sub>O were determined according to the standard procedures (Schweins et al., 1996).

## Acknowledgment

We thank Alfred Wittinghofer, Matthias Geyer, and Hans-Robert Kalbitzer for valuable discussion. We also thank Jan Florian and Ingo Muegge for discussion and Tim Glennon for critically reading the manuscript.

## REFERENCES

- Adamo, C., & Lelj, F. (1995) *Int. J. Quantum Chem.* 56, 645–653.
- Admiraal, S. J., & Herschlag, D. (1995) *Chem. Biol.* 2, 729–739.
- Albery, W. J. (1980) *Annu. Rev. Phys. Chem.* 31, 227.
- Åqvist, J., & Warshel, A. (1993) *Chem. Rev.* 93, 2523–2544.
- Åqvist, J., & Hansson, T. (1996) *J. Phys. Chem.* 100 (in press).
- Åqvist, J., Medina, C., & Samuelson, J.-E. (1994) *Protein Eng.* 7, 385–391.
- Brownbridge, G. G., Lowe, P. N., Moore, K. J., Skinner, R. H., & Webb, M. (1993) *J. Biol. Chem.* 268, 10914–10919.
- Cleland, W. (1990) *Enzymes* 19, 99–158.
- Davis, A. M., Hall, A. D., & Williams, A. (1988) *J. Am. Chem. Soc.* 110, 5105–5108.
- Eccleston, J. F., & Webb, M. R. (1982) *J. Biol. Chem.* 257, 5046–5049.
- Fersht, A. R. (1984) *Enzyme, Structure and Mechanism*, 2nd ed., Freeman, New York.
- Fersht, A. R., Leatherbarrow, R. J., & Wells, T. N. C. (1986) *Nature* 322, 284–286.
- Feuerstein, J., Goody, R. S., & Webb, M. R. (1989) *J. Biol. Chem.* 264, 6188–6190.
- Fisher, A. J., et al. (1995) *Biochemistry* 34, 8960.
- Fothergill, M., Goodman, M. F., Petruska, J., & Warshel, A. (1995) *J. Am. Chem. Soc.* 117, 11619–11627.
- Gerlt, J. A., & Gassman, P. G. (1993) *J. Am. Chem. Soc.* 115, 11552–11568.
- Goody, R. S. (1994) *Nature* 372, 220.
- Guthrie, J. P. (1977) *J. Am. Chem. Soc.* 99, 3991–4001.
- Guthrie, J. P. & Kluger, R. (1993) *J. Am. Chem. Soc.* 115, 11569–11572.
- Hammitt, L. P. (1937) *J. Am. Chem. Soc.* 59, 96.
- Hammond, G. S. (1955) *J. Am. Chem. Soc.* 77, 334.
- Hollfelder, F., & Herschlag, D. (1995) *Biochemistry* 34, 12255–12264.
- Hrouda, V., Florián, J., Polásek, M., & Hobza, P. (1994) *J. Phys. Chem.* 98, 4742–4747.
- Hwang, J. K., & Warshel, A. (1987) *J. Am. Chem. Soc.* 109, 715.
- Hwang, J. K., King, G., Creighton, S., & Warshel, A. (1988) *J. Am. Chem. Soc.* 110, 5297.
- Jencks, W. P. (1987) *Catalysis in Chemistry and Enzymology*, Dover Public, New York.
- Jencks, W. P., & Salvesen, K. (1971) *J. Am. Chem. Soc.* 93, 4433.
- King, G., & Warshel, A. (1989) *J. Chem. Phys.* 91, 3647–3661.
- Kong, Y. S., & Warshel, A. (1995) *J. Am. Chem. Soc.* 117, 6234–6242.
- Kreevoy, M. M., & Kotchevar, A. T. (1990) *J. Am. Chem. Soc.* 112, 3579.
- Kuharski, R. A., Bader, J. S., Chandler, D., Sprik, M., Klein, M., & Impey, R. W. (1988) *J. Chem. Phys.* 89, 9219.
- Langen, R., Schweins, T., & Warshel, A. (1992) *Biochemistry* 31, 8691–8696.
- Leffler, J. E., & Grunwald, E. (1963) *Rates and Equilibria of Organic Reactions*, Wiley & Sons, New York.

- Maegley, K. A., Admiral, S. J., & Herschlog, D. (1996) *Proc. Natl. Acad. Sci. U.S.A.* 93, 8160–8166.
- Marcus, R. A. (1964) *Annu. Rev. Phys. Chem.* 15, 155.
- Marcus, R. A. (1968) *J. Phys. Chem.* 72, 891.
- Mittal, R., Ahmadian, M. R., Goody, R. S., & Wittinghofer, A. (1996) *Science* 273, 115.
- Papazyan, A., & Maroncelli, M. (1991) *J. Chem. Phys.* 95, 9219.
- Pross, A., & Shaik, S. S. (1983) *Acc. Chem. Res.* 16, 363.
- Ren, X., Tu, C., Laipis, P. J., & Silverman, D. N. (1995) *Biochemistry* 34, 8492–8498.
- Schowen, K. B., & Schowen, R. L. (1982) *Methods Enzymol.* 87, 551.
- Schweins, T., Langen, R., & Warshel, A. (1994) *Nature Struc. Biol.* 1, 476–484.
- Schweins, T., Geyer, M., Scheffzek, K., Warshel, A., Kalbitzer, H. R., & Wittinghofer, A. (1995) *Nat. Struct. Biol.* 2, 36–44.
- Schweins, T., Geyer, M., Kalbitzer, H. R., Wittinghofer, A., & Warshel, A. (1996) *Biochemistry* 35, xxxxx–xxxxx.
- Sondek, J., Lambright, D. G., Noel, J. P., Hamm, H. E., & Sigler, P. B. (1994) *Nature* 372, 276–279.
- Toney, M. D., & Kirsch, J. F. (1989) *Science* 243, 1485–1488.
- Warshel, A. (1984) *Pontif. Acad. Sci. Script. Varia.* 55, 59.
- Warshel, A. (1991) *Computer Modeling of Chemical Reactions in Enzyme and Solutions*, Wiley & Sons, New York.
- Warshel, A., & Weiss, R. M. (1980) *J. Am. Chem. Soc.* 102, 6218.
- Warshel, A., Hwang, J. K., & Åqvist, J. (1992) *Faraday Discuss.* 93, 225–238.
- Warshel, A., Schweins, T., & Fothergil, M. (1994) *J. Am. Chem. Soc.* 116, 8437–8442.
- Yadav, A., Jackson, R., Holbrook, J. J., & Warshel, A. (1991) *J. Am. Chem. Soc.* 113, 4800–4805.

BI961119G